Stem Cell Reports
Report
OPEN ACCESS

Hemogenic Endothelial Cells Can Transition to Hematopoietic Stem Cells through a B-1 Lymphocyte-Biased State during Maturation in the Mouse Embryo

Michihiro Kobayashi,[1] Stefan P. Tarnawsky,[2] Haichao Wei,[1] Akansha Mishra,[2] Nathalia Azevedo Portilho,[1] Pamela Wenzel,[1] Brian Davis,[1] Jiaqian Wu,[1] Brandon Hadland,[3,4] and Momoko Yoshimoto[1,*]
[1]Center for Stem Cell and Regenerative Medicine, Institute of Molecular Medicine, McGovern Medical School, University of Texas Health Science Center at Houston, Houston, TX 77030, USA
[2]Wells Center for Pediatric Research, Department of Pediatrics, Indiana University School of Medicine, Indianapolis, IN 46202, USA
[3]Clinical Research Division, Fred Hutchinson Cancer Research Center, Seattle, WA 98109, USA
[4]Department of Pediatrics, Division of Pediatric Hematology/Oncology, University of Washington School of Medicine, Seattle, WA 98105, USA
*Correspondence: momoko.yoshimoto@uth.tmc.edu
https://doi.org/10.1016/j.stemcr.2019.05.025

SUMMARY

Precursors of hematopoietic stem cells (pre-HSCs) have been identified as intermediate precursors during the maturation process from hemogenic endothelial cells to HSCs in the aorta-gonad-mesonephros (AGM) region of the mouse embryo at embryonic day 10.5. Although pre-HSCs acquire an efficient adult-repopulating ability after *ex vivo* co-culture, their native hematopoietic capacity remains unknown. Here, we employed direct transplantation assays of CD45$^-$VE-cadherin(VC)$^+$KIT$^+$(V$^+$K$^+$) cells (containing pre-HSCs) into immunodeficient neonatal mice that permit engraftment of embryonic hematopoietic precursors. We found that freshly isolated V$^+$K$^+$ cells exhibited significantly greater B-1 lymphocyte-biased repopulating capacity than multilineage repopulating capacity. Additionally, B cell colony-forming assays demonstrated the predominant B-1 progenitor colony-forming ability of these cells; however, increased B-2 progenitor colony-forming ability emerged after co-culture with Akt-expressing AGM endothelial cells, conditions that support pre-HSC maturation into HSCs. Our studies revealed an unexpected B-1 lymphocyte bias of the V$^+$K$^+$ population and acquisition of B-2 potential during commitment to the HSC fate.

INTRODUCTION

The formation of the first hematopoietic stem cells (HSCs) in the aorta-gonad-mesonephros (AGM) region of the mouse embryo is considered a stepwise maturation process of precursor cells from hemogenic endothelial cells (HECs) to HSCs through intermediate stages (Hadland and Yoshimoto, 2018). At embryonic day 10.5 (E10.5), these intermediate precursors of HSCs (referred to as pre-HSCs) are included in the CD45$^-$VE-cadherin(VC)$^+$KIT$^+$ population (type I pre-HSCs) and acquire adult-repopulating ability only after *ex vivo* aggregation cultures with OP9 cells or co-culture with either Akt-expressing endothelial cells (AGM-ECs) or delta-like-1-expressing OP9 cells (Hadland et al., 2015; Rybtsov et al., 2011; Zhou et al., 2016). At E11.5, adult-repopulating ability is detected in the CD45$^+$VC$^+$KIT$^+$ population (type II pre-HSCs) at a low frequency, but becomes efficient following the *ex vivo* cultures indicated above. Therefore, these *ex vivo* cultures are thought to reflect the maturation process *in vivo*, whereby pre-HSCs become HSCs, rapidly expand, and subsequently seed the fetal liver (FL) at E12.5.

Separately, neonatal-repopulating HSCs have been identified as early as E9 in both the yolk sac (YS) and para-aortic splanchnopleura (P-Sp, referred to as AGM after E10) region, as specific HSCs that can engraft only in preconditioned neonatal mice, but not in adult mice. The residual fetal environment in the neonatal liver is considered to be permissive for engraftment of embryonic hematopoietic precursors (Arora et al., 2014; Yoder et al., 1997). E10.5 CD45$^-$VC$^+$ cells are reported to engraft in SCID neonates (although at very low chimerism) (Fraser et al., 2002). Thus, type I pre-HSCs and neonatal-repopulating HSCs are overlapping populations, and neonatal mice provide a powerful tool to evaluate the repopulating capacity of freshly isolated embryonic hematopoietic precursors by direct transplantation assays.

Prior to HSC emergence in the AGM region at E10–E11, lymphoid potential is detected in the YS and P-Sp region. We found that B progenitors derived from HECs in the E9 YS and P-Sp *in vitro* culture provide peritoneal B-1 and splenic marginal zone (MZ) B cell engraftment (but not B-2 cell) upon transplantation into NOD/SCID/Il2rγc$^{-/-}$ (NSG) neonates (Yoshimoto et al., 2011). B-1 cells are a unique innate-like B cell subset separated from conventional HSC-derived adoptive B (B-2) cells, arise during embryonic development, and play important roles in the first line of defense by secreting natural antibodies (Hardy and Hayakawa, 1991; Hayakawa et al., 1983). MZ B cells belong to the B-2 lineage, but a part of MZ B cells are fetal derived (Carey et al., 2008; Yoshimoto et al., 2011). The origin of CD5$^+$ B-1a cells has been controversial because highly

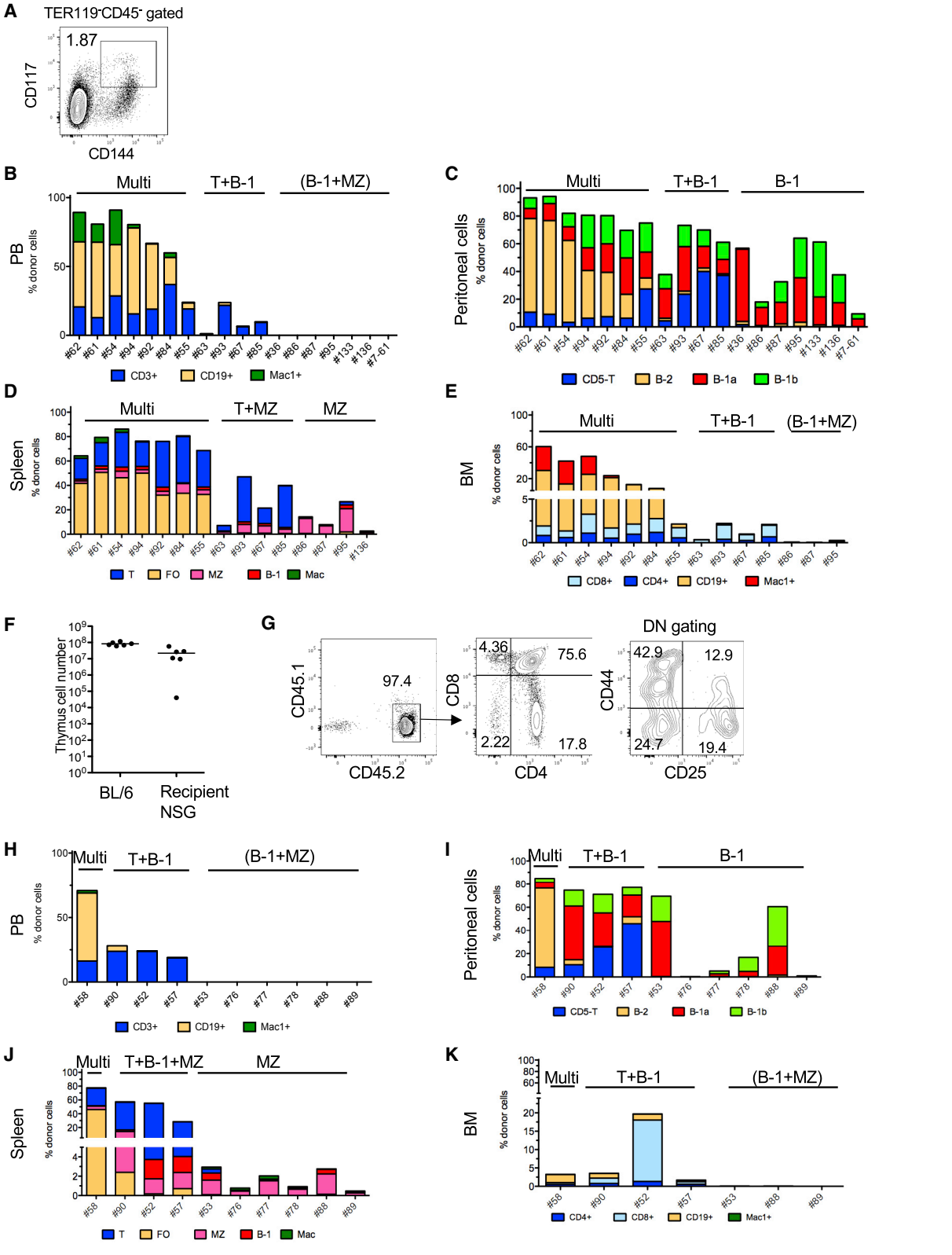

(legend on next page)

purified long-term (LT)-HSCs in the E15 FL and adult bone marrow (BM) failed to repopulate the peritoneal B-1a cells (Ghosn et al., 2012, 2016), whereas a barcoding study indicated that B-1a cells were produced by E14 FL HSC transplantation (Kristiansen et al., 2016). However, it is commonly observed that FL LT-HSCs produce mainly B-2 cells upon transplantation, although the FL is a major source of B-1a cells. This discrepancy suggests that the B-1a precursors residing in the FL are not produced by LT-HSCs but by precursors at earlier embryonic stages. Accordingly, we reported the presence of an HSC-independent developmental pathway of B-1a cells in an HSC-deficient mouse model (Kobayashi et al., 2014). Thus, it remains unresolved whether B-1a cells are produced by HSCs at the fetal stage. Because FL LT-HSCs produce mainly B-2 cells, it is assumed that pre-HSCs and the first HSCs in the AGM region are also B-2 biased.

Our group demonstrated that single pre-HSCs derived from E9.5–E11.5 P-Sp/AGM region, following co-culture with AGM-ECs, provide multilineage engraftment including both B-1a and B-2 cells in lethally irradiated mice (Hadland et al., 2017). These data suggested that B-1a cells and HSCs had a shared clonal origin from E9.5–E11 pre-HSCs. However, previous studies of type I pre-HSCs relied upon *ex vivo* co-cultures to evaluate their adult-repopulating ability. Therefore, it remains unknown whether freshly isolated pre-HSCs have the inherent ability to produce both B-1a repopulating cells and multipotent HSCs (with or without B-1a cell potential) or alternatively acquire these abilities subsequent to their maturation to HSCs.

To address this specific question, we examined the hematopoietic activity of freshly isolated E10.5 $CD45^{-}VC^{+}KIT^{+}$ cells (hereafter referred to as $V^{+}K^{+}$ cells) by transplantation assays into NSG neonates. Surprisingly, highly purified endothelial protein C receptor $(EPCR)^{hi}V^{+}K^{+}$ cells did not display multilineage repopulating ability but B-1-biased repopulating ability. Moreover, the $EPCR^{hi}V^{+}K^{+}$ population obtained B-2 progenitor colony-forming ability following co-culture with AGM-ECs, whereas it originally had an exclusive B-1 progenitor colony-forming ability. Based on these results, we conclude that E10.5 $V^{+}K^{+}$ cells natively possess B-1-biased repopulating capacity and gain B-2 progenitor potential upon their maturation to adult-engrafting HSCs.

RESULTS

E10.5 $V^{+}K^{+}$ Population Contains B-1-Biased and Multilineage Repopulating Cells in Immunodeficient Neonates

The E10.5 $V^{+}K^{+}$ population containing pre-HSCs rarely engrafts in lethally irradiated adult mice when transplanted directly (Rybtsov et al., 2011). Because neonatal mice provide a more permissive environment for hematopoietic reconstitution by embryo-derived cells (Arora et al., 2014; Yoder et al., 1997; Yoshimoto et al., 2011), the $V^{+}K^{+}$ cells ($CD117^{+}CD144^{+}$cells) isolated from the E10.5 AGM region were injected into sublethally irradiated NSG neonates to assess their direct engraftment potential (1.8 embryo equivalent [e.e.] to 10 e.e.) (Figure 1A). Additional surface markers were used to refine the identity of the population, including CD41, CD43, CD11a, and EPCR (Table S1 and Figure S1A) (Batsivari et al., 2017; Hadland et al., 2017; Inlay et al., 2014; Zhou et al., 2016). The donor cell percentage and lineage contributions in the peripheral blood (PB) were assessed at 16-weeks post transplantation (Figures 1B and S1B). Among the total of 30 recipient mice, donor cells were detected in the PB of 11 mice. Seven mice exhibited multilineage repopulation (T, B, and myeloid cells) and four mice showed T cell-dominant repopulation in the PB. Multilineage repopulation included T cells and all subsets of B cells, including B-2 and B-1 cells in the peritoneal cavity (Figures 1C and S1C) and follicular (FO) and MZ B cells in the spleen (Figures 1D and S1E). Multilineage engraftment was also confirmed in the recipient BM and spleen (Figures 1D, 1E, and S1D). Importantly, the thymus was reconstituted in six out of seven recipients with multilineage repopulation (Figure 1F). Donor cells in the repopulated thymus included CD4, CD8 single-positive, double-positive, and double-negative (DN) populations including DN1 to DN4 (Figure 1G). Surprisingly, four mice showing T cell-dominant repopulation in the PB displayed donor-derived peritoneal B-1 and splenic MZ B cells

Figure 1. Pre-HSCs Displayed a Diversity of Hematopoietic Repopulating Ability in the NSG Neonates

(A–E) Fluorescence-activated cell sorting (FACS) plots (A) for gating of $PI^{-}TER119^{-}CD45^{-}CD144$(VE-cadherin, VC)$^{+}KIT(CD117)^{+}$ ($V^{+}K^{+}$) population from E10.5 AGM. The $V^{+}K^{+}$ population plots are representative of more than 10 experiments. E10.5 AGM donor-derived cell percentage and lineages in the recipient peripheral blood (PB) (B), peritoneal cells (C), spleen (D), and BM (E) are depicted.

(F) Cell number in the thymus of non-transplanted BL/6 (BL/6, n = 6) and NSG mice with multilineage reconstitution by E10.5 $V^{+}K^{+}$ cells (recipient NSG, n = 6).

(G–K) AGM pre-HSC-derived T cells in the recipient thymus (G) are shown. Representative FACS plots are depicted among six thymus-repopulated mice. E10.5 YS donor-derived percentage and lineages in the recipient PB (H), peritoneal cells (I), spleen (J), and BM (K) are depicted. All the hematopoietic tissues of recipient mice were analyzed at 4–6 months after transplantation.

Reconstituted cell population (Multi, T + B-1, B-1 + MZ) is depicted in each graph based on the overall results.

but not FO B (B-2) cells (T + B-1 + MZ repopulation) (Figures 1B–1D and S1B–S1E). Only one out of four NSG mice with T + B-1 + MZ repopulation had a reconstituted thymus. Furthermore, in seven recipient mice with no donor cells in the PB, donor-derived peritoneal B-1 and splenic MZ B cells, but not FO B cells, were detected (Figures 1B–1D and S1B–S1E). Thus, the E10.5 AGM V^+K^+ cells contained three types of repopulating cells: multilineage, T + B-1(+MZ)-biased, and B-1 + MZ-biased, suggesting inherent heterogeneity in this population known to contain pre-HSCs. Importantly, this study identified the earliest transplantable B-1a precursors by direct transplantation; however, this approach did not distinguish whether multilineage repopulation including peritoneal B-1a cells was derived from a single precursor cell or two or more distinct precursors (such as multilineage pre-HSCs lacking B-1a potential and B-1-biased pre-HSCs), as recipients received $\geq$1.8 e.e. donor cells (Table S1).

The V^+K^+ Population in the E10.5 YS Also Contains B-1-Biased and Multilineage Neonatal-Repopulating Cells

The V^+K^+ cells sorted from E10.5 YS (2.8 e.e. to 10 e.e.) was also injected into sublethally irradiated NSG neonates (Table S1). Among the total of 23 recipient mice, donor-derived cells were detected in the PB of four mice at 16 weeks post transplantation (Figure 1H). Only one mouse exhibited multilineage repopulation (mouse #58), and three mice displayed T cell-dominant engraftment (mouse #52, 57, 90) (Figure 1H). The mouse exhibiting multilineage repopulation in the PB harbored donor-derived T cells, dominant B-2 cells, and relatively fewer B-1 cells in the peritoneal cavity (Figure 1I), and predominant FO B cells in the spleen (Figure 1J). Mice with T-dominant repopulation harbored peritoneal B-1 cells and splenic MZ B cells, but very few B-2 cells (Figures 1I and 1J). Among the mice with no donor cells in the PB, six mice exhibited only B-1 and MZ B cell repopulation in the peritoneal cavity and spleen. Thus, similar to the AGM, the YS-derived V^+K^+ cells also contained multilineage, T + B-1 + MZ-biased, and B-1 + MZ-biased repopulating cells.

The V^+K^+ Population Contains More B-1-Biased Repopulating Cells Than Multilineage Neonatal-Repopulating Cells

Limiting dilution analysis calculated the frequency of multilineage repopulating cells among $V^+K^+CD41^+$ cells as 1 out of 10.1 e.e. in the E10.5 AGM, whereas B-1a cells were repopulated in all recipient mice by this cell population even when only 2.3 e.e. was injected (Figure 2A and Table S1). EPCR, which greatly enriches for pre-HSC activity (Hadland et al., 2017; Zhou et al., 2016), was included as an additional marker to examine the frequency of B-1 and multilineage repopulating cells in the enriched population; ten $EPCR^{hi}CD41^{dim}V^+K^+$ cells from E10.5 AGM were injected into sublethally irradiated NSG neonates (Figure 2B). Although no multilineage engraftment was observed, donor-derived peritoneal B-1 and splenic MZ B cells were present in two of five recipient mice at 4 months post transplantation (Figures 2C–2E). This result indicates that the main population among $EPCR^{hi}CD41^{dim}V^+K^+$ cells was B-1-biased repopulating cells.

We also compared the B cell subsets repopulated by highly purified E15 FL LT-HSCs (defined as $CD150^+CD48^-lin^-SCA1^+KIT^+$ cells) and multipotent progenitors (MPPs) ($CD150^-CD48^+lin^-$ $SCA1^+KIT^+$ cells) transplanted into NSG neonates (Figure S2A). As reported by Ghosn et al. (2016), we confirmed that E15 FL LT-HSCs predominantly repopulated B-2 cells and a very low percentage of B-1a cells while MPPs repopulated both B-1a and B-2 cells (Figures 2F, 2G, S2B, and S2C).

Taken together, these data indicated that when assayed by direct neonatal transplantation with limiting cell numbers, the $EPCR^{hi}CD41^{dim}V^+K^+$ population harbored exclusive B-1-biased repopulating capacity rather than multilineage repopulating capacity, revealing an unexpected lineage bias of pre-HSCs that is distinct from the FL LT-HSCs, which are the functionally mature progeny of pre-HSCs. These findings suggest that a critical component of the maturation of pre-HSCs to LT-HSCs may involve the acquisition of B-2 lymphoid and multilineage repopulation capacity.

HSC-Specific Genes Are Rarely Expressed in the V^+K^+ Cells at a Single-Cell Level

Since the frequency of multilineage repopulating cells among the V^+K^+ population by direct neonatal transplantation assays was extremely low in our results, we sought to examine whether this observation corresponds with hematopoietic specific gene expression profiles at the single-cell level. We utilized single-cell RNA-sequencing (scRNA-seq) data (Baron et al., 2018) (downloaded from GEO: GSE112642) derived from E10 intra-aortic hematopoietic clusters (IAHCs: KIT^+, $CD31^+$, *Gpr56*$^+$) and endothelial-hematopoietic transition cells (EHTs: $CDH5^+$, *Gfi1*$^+$, KIT^+), which include pre-HSCs that overlap with the E10.5 V^+K^+ cells in our study based on common cell-surface markers. t-SNE (t-Distributed stochastic neighbor embedding) analysis of these two populations demonstrated mapping similar to that reported by Baron et al. (2018); further analysis using RaceID3, a computational algorithm to identify rare cell types, found five main clusters among the IAHC and EHT populations (Figure S3). In our analysis, cluster 3 was enriched with essential genes associated with pre-HSC markers including *Cdh5*, *Pecam1*, and

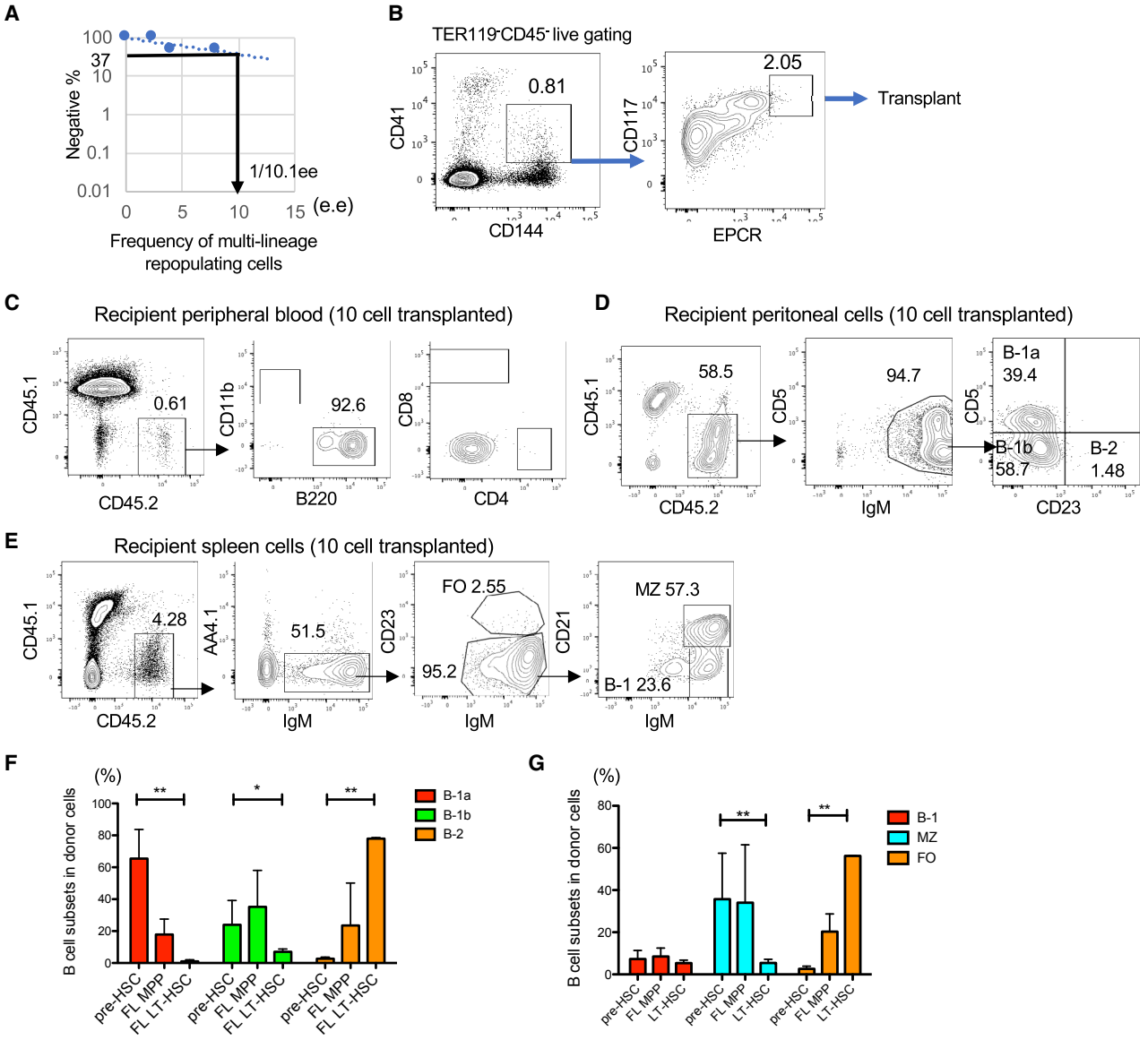

Figure 2. The B-1-Biased Repopulating Cells Are the Main Population among the E10.5 AGM V^+K^+ Population

(A) Frequency of multilineage repopulating cells was calculated based on limiting dilution analysis. The number of mice transplanted with $CD41^{dim}V^+K^+$ cells was counted for the analysis.

(B–G) Gating strategy of $EPCR^{hi}CD45^-CD117(KIT)^+CD144(VC)^+CD41^{dim}$ ($EPCR^{hi}VK^+CD41^{dim}$) cells from E10.5 AGM (B). Ten $EPCR^{hi}VK^+CD41^{dim}$ cells were transplanted into five NSG neonates. No donor cells were detected in the PB of three mice, but a small percentage of donor-derived B cells was detected in the PB in two recipient mice at 4 months after transplantation (C). In these two mice, the peritoneal B-1 cells and splenic MZ B cells were well repopulated while no other lineages were detected (D and E). Percentage of each B cell subset among immunoglobulin M $(IgM)^+$ B cells in the peritoneal cavity (F) and spleen (G) of recipient NSG mice at 6 months post transplantation with E10.5 AGM V^+K^+ cells (shown as pre-HSCs) (n = 10), E15 FL LT-HSCs (n = 3), and MPP (n = 3). *$p < 0.05$, **$p < 0.01$.

hematopoiesis/HSC-generation including *Mecom* (*Evi1*) and *Vwf* (Table S2). However, HSC-specific genes including *Hoxb5*, *Fgd5*, and *Pdzk1ip1* were only expressed in a few cells and not co-expressed in the same cell (Figure S3). These data are consistent with the very low frequency of neonatal-repopulating cells among the V^+K^+ population. Of note, there are caveats; HSC-specific genes are not always highly expressed in HSCs and due to the limitation of the read counts in scRNA-seq analysis, no or low expression of a gene does not mean that the cell does not express the gene at all. Therefore, there may be missing cells that express HSC-specific genes, which were not detected in this analysis.

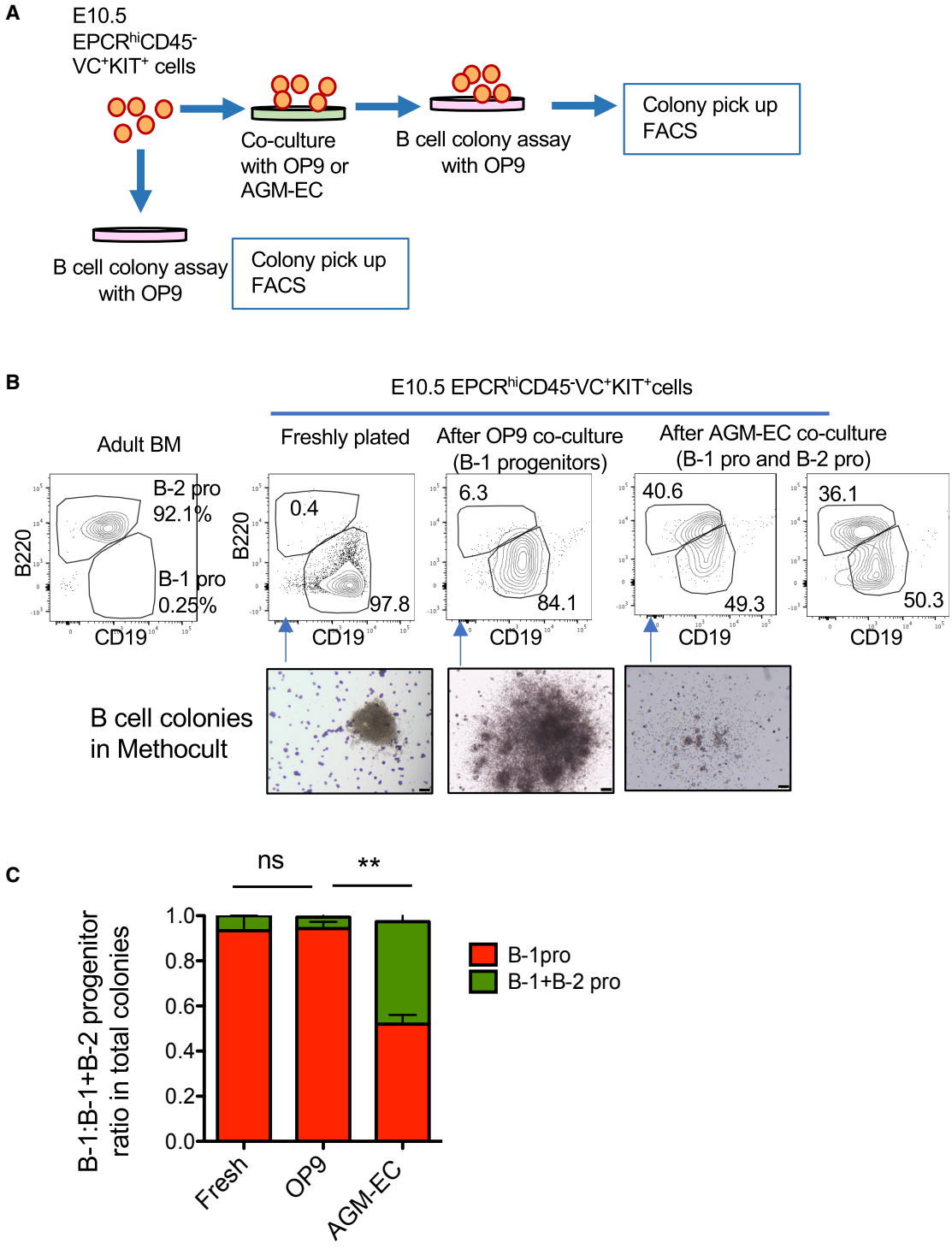

Figure 3. B-1-Biased V$^+$K$^+$ Cells Gain B-2 Potential following *In Vitro* Co-culture with AGM-EC

(A) Experimental procedure for B cell colony-forming assays. E10.5 V$^+$K$^+$ population was plated into methylcellulose (MTC) (Methocult) with 1 × 10^5 OP9 cells directly or after co-culture with OP9 or AGM-EC for 5 days. Eight to 11 days after initiating MTC culture the colony number was counted, and each colony was picked up for FACS analysis.

(legend continued on next page)

AGM-EC Co-culture Enhances B-2 Potential from the B-1-Biased Population

Although our current studies demonstrated that the V^+K^+ population contained predominantly B-1-biased repopulating cells, our group demonstrated that single pre-HSCs after AGM-EC co-culture produced both B-1a and B-2 lymphocyte engrafting cells upon transplantation (Hadland et al., 2017). Therefore, we hypothesized that during their maturation to HSCs in AGM-EC co-culture, B1-biased pre-HSCs gain B-2 potential. To test this hypothesis, we examined clonal B-1 and B-2 progenitor production from the E10.5 $EPCR^{hi}V^+K^+$ cells *in vitro*, utilizing a modified semisolid methylcellulose (MTC) culture (Montecino-Rodriguez et al., 2016) (Figure 3A). B-1- or B-2-specific progenitors are identified as $AA4.1^+CD19^+B220^{lo\text{-}neg}$ and $AA4.1^+CD19^-B220^+$ cells, respectively, by cell-surface markers of the colonies in the MTC culture (Figure 3B). First, freshly isolated $EPCR^{high}V^+K^+$ cells from E10.5 AGM were confirmed to form almost exclusively B-1 progenitor colonies (Figures 3B and 3C). Next, the $EPCR^{hi}V^+K^+$ cells were co-cultured with either OP9 cells or AGM-ECs for 5 days, and $CD11b^-CD45^+$ cells were sorted and replated in the MTC culture with OP9 cells (Figure 3A). While the $EPCR^{hi}V^+K^+$ cells co-cultured with OP9 cells formed primarily B-1 progenitor colonies, the same population co-cultured with AGM-ECs produced significantly more colonies containing both B-1 and B-2 progenitors than colonies containing only B-1 progenitors (Figures 3B and 3C). This result suggested that the B-1-biased precursors acquired B-2 progenitor potential after AGM-EC co-culture. This is consistent with our current and previous transplantation data showing that freshly isolated V^+K^+ cells repopulate primarily B-1 cells in the immunodeficient neonates, while AGM-EC co-culture endows single V^+K^+ cells with multilineage repopulating ability, including both B-1a and B-2 cells in adult recipients. Taken together, our study supports a model in which the acquisition of B-2 potential corresponds with the maturation of B-1-biased pre-HSCs to multilineage adult-repopulating HSCs (Figure 4).

DISCUSSION

In the present study, we demonstrated the unexpected presence of predominant B-1- and MZ B-biased (and occasionally T-biased) repopulating cells in the E10.5 V^+K^+ population. Rare neonatal multilineage repopulating cells are detectable, as might be expected from a maturing HSC precursor. Furthermore, the $EPCR^{hi}V^+K^+$ cells, which are highly enriched with pre-HSC activity, displayed exclusive B-1 progenitor colony-forming ability *in vitro* and B-1-biased repopulating activity *in vivo* when transplanted at limiting numbers. Conversely, this population after co-culture with AGM-EC showed B-1 + B-2 progenitor colony-forming activity *in vitro* and adult multilineage repopulating activity *in vivo* (Hadland et al., 2017). These results led us to propose a model in which E10.5 pre-HSCs innately possess B-1-biased repopulating capacity that may represent a "snapshot" of the developmental process of pre-HSC maturation to adult-repopulating HSCs with B-2 potential *in vivo* (Figure 4).

In agreement with a previous report (Ghosn et al., 2016), we confirmed that E15 FL LT-HSCs failed to efficiently repopulate B-1a cells, whereas a recent barcoding study showed E14 FL HSC-derived B-1a cells (Kristiansen et al., 2016). One scenario to reconcile these findings is that the first HSCs retain the B-1a-producing ability inherent to pre-HSCs, but gradually lose it upon acquisition of B-2 and HSC potential. Alternatively, FL HSCs with B-1a potential derived from B-1-biased pre-HSCs may represent the "developmentally restricted HSCs" reported by Beaudin et al. (2016), distinct from adult HSCs. Given assay limitations, we cannot entirely exclude the possibility that B-1-biased precursors at E10.5 and multilineage repopulating HSCs at later stages represent distinct populations derived from separate lineages. Clarification of the relationship between HSCs and B-1a cells will require *in vivo* clonal assays and B-1-specific lineage tracing.

In summary, we demonstrated that the E10.5 V^+K^+ cells are a heterogeneous population containing three types of repopulating cells (multilineage, T + B-1 + MZ, and only B-1 + MZ), and that the earliest B-1- and MZ-biased (and T-biased) repopulating cells are the main population. It would be important to identify cell-surface markers to segregate these precursor populations. Additionally, because B-2 and thymic repopulation are essential aspects of HSC engraftment, acquisition of B-2 potential may be a critical and defining step in the development of pre-HSCs to adult-repopulating HSCs. Further in-depth analysis of the transcriptional and epigenetic properties of the V^+K^+ population at the single-cell level will be required to identify the molecular mechanisms mediating this heterogeneity in inherent repopulation capacity during the transition from a B-1-biased to a B-2/multilineage state.

(B) Representative colony FACS plots and colony photos. Adult BM FACS plot (left) represents $lin^-IgM^-AA4.1^+$ gated B progenitors from freshly isolated BM cells. Scale bars, 200 μm.

(C) Ratio of only B-1 progenitor colonies and B-1 + B-2 progenitor colonies to total colonies of pre-HSCs after co-culture with OP9 or AGM-EC. Colony assays were performed in triplicates for each culture condition, and repeated three times. $^{**}p < 0.01$; ns, not significant.

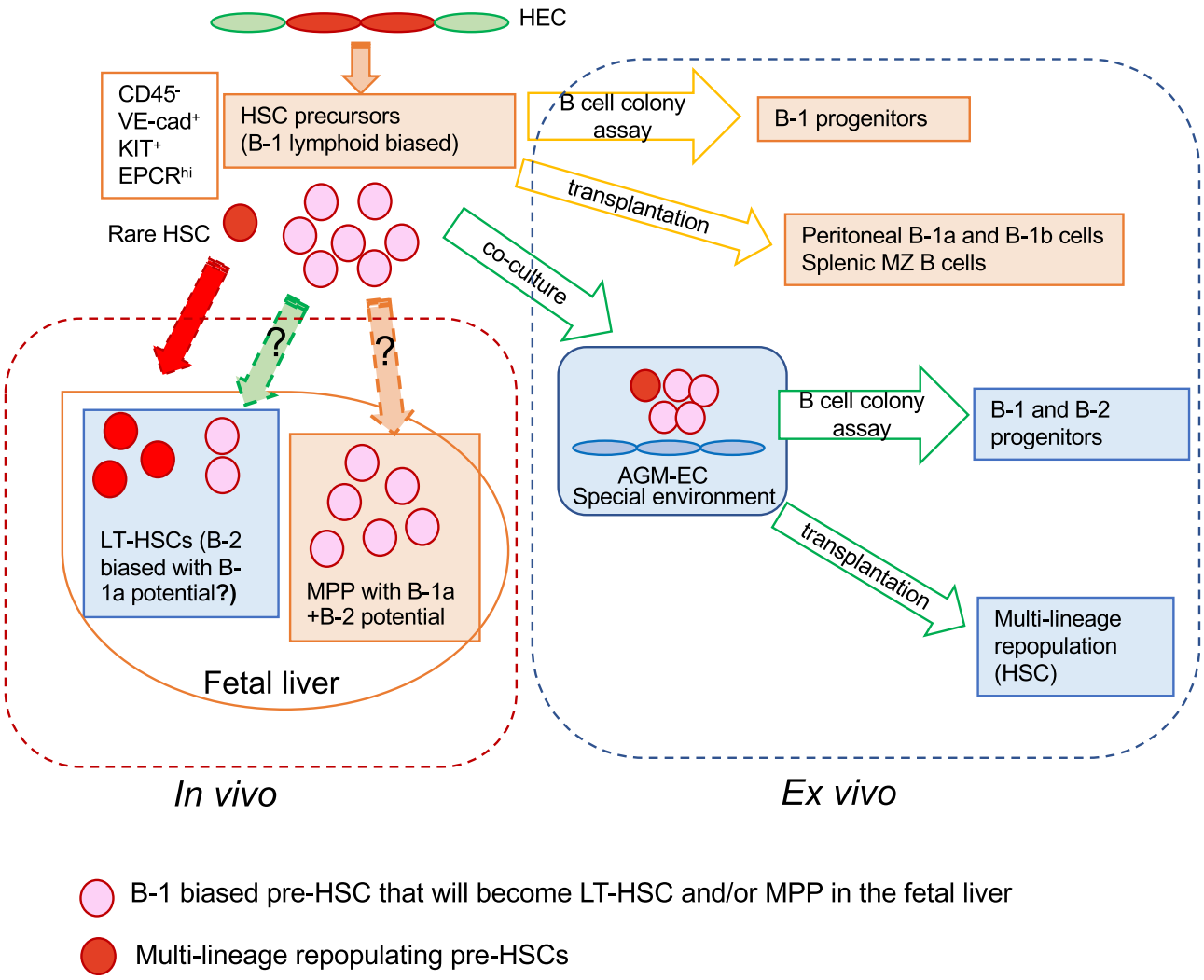

Figure 4. Hemogenic Endothelial Cell Transition through B-1-Biased State to Become HSCs (Working Model)
A full explanation is provided in the main text. MPP, multipotent progenitors.

EXPERIMENTAL PROCEDURES

Mice

C57BL/6 and NSG mice were used for timed pregnancy, as donors and recipients, respectively. Embryo age was also confirmed by counting the somite numbers. All the mice were maintained in specific pathogen-free conditions at the University of Texas Health Science Center at Houston, following approved IACUC protocols.

Cell Preparation and Cell Sorting

YS and AGM tissues were dissected and digested in 0.25% collagenase (STEMCELL Technologies) for 30 min at 37°C, followed by addition of cell dissociation buffer (Life Technologies) and preparation of a single-cell suspension. For FL LT-HSCs and MPPs, FL was harvested and made into a single-cell suspension. Mononuclear cells were collected after centrifugation on Histopaque (Sigma) at 1,500 rpm for 30 min. Cell number was counted with trypan blue and cells were stained with the antibodies for fluorescence-activated cell sorting (Supplemental Experimental Procedures).

Transplantation

Day-1 to -3 NSG neonates (express CD45.1) were used as recipients and were irradiated with 150 rad before transplantation. Donor cells (CD45.2) were injected into the facial vein. Blood was taken every month from the 4th week after transplantation and donor cell types were examined by flow cytometry (LSRII, Becton Dickinson).

Limiting Dilution Analysis

The frequencies of B-1 biased progenitors and multilineage repopulating cells were calculated by limiting dilution analysis. The recipient mice transplanted with CD41^{dim}V^{+}K^{+} cells were counted.

The frequency of the progenitor was determined from 37% of the negative fraction according to Poisson distribution.

Modified Semisolid Clonal Culture and Single-Colony Flow-Cytometry Analysis

We optimized the semisolid culture system developed by Dorshkind's group (Montecino-Rodriguez et al., 2016). Pre-HSCs were sorted and co-cultured with OP9 or AGM-ECs with 10 ng/mL interleukin-7 (IL-7) and Flt3-ligand. After 5 days of co-culture, $lin^{-}CD45^{+}$ cells were sorted from each co-culture, mixed with 1×10^{5} OP9 cells, and plated into 35-mm Petri dishes in Methocult M3630 in triplicate (containing IL-7, STEMCELL Technologies) with 10 ng/mL Flt3 ligand. Around days 8–11, the colony number per dish was counted. Each colony was picked up under the inverted microscope and then stained with antimouse AA4.1, CD19, B220, and CD11b, followed by flow-cytometric analysis on LSRII (Becton Dickinson).

Statistical Analysis

The unpaired, two-tailed Student's t test was used for statistical analysis.

Single-Cell RNA-Sequencing Analysis

The single-cell data of IAHC and EHT cells were downloaded from GEO: GSE112642 (Baron et al., 2018). As described in the report by Baron et al. (2018), the data analysis was performed using RaceID3_StemID2 (https://github.com/dgrun/RaceID3_StemID2). We employed k-medoids clustering of the correlation matrix with five clusters as inferred by the gap statistic. The expression cutoff for the identification of outlier genes was 10. The minimal number of outlier genes required to identify a cell as an outlier was 10. When a parameter was not specified, the default value was used. The significant differentially expressed genes of each cluster were identified (in which p values are calculated using negative binomial distribution and corrected for multiple testing by the Benjamini-Hochberg method).

SUPPLEMENTAL INFORMATION

Supplemental Information can be found online at https://doi.org/10.1016/j.stemcr.2019.05.025.

AUTHOR CONTRIBUTIONS

Conceptualization, M.Y.; Methodology, M.Y., J.W., and H.W.; Investigation, M.Y., M.K., S.P.T., H.W., A.M., and N.A.P.; Formal Analysis, H.W. and J.W.; Writing – Original Draft, M.Y.; Writing – Review & Editing, M.Y., B.H., B.D., S.P.T., P.W., H.W., and J.W.; Resources, B.H., P.W., and J.W.; Funding Acquisition, M.Y. and B.H.; Supervision, M.Y. and M.K.

ACKNOWLEDGMENTS

This work is supported by NIAID R01AI121197 (M.Y.) and NHLBI K08HL140143 (B.H.). J.W. and H.W. were supported by grants from the NIH R01 NS088353, R21EY028647, and R21AR071583; The Staman Ogilvie Fund-Memorial Health Foundation; Mission Connect, a program of the TIRR Foundation.

Received: February 24, 2019
Revised: May 24, 2019
Accepted: May 24, 2019
Published: June 20, 2019

REFERENCES

Arora, N., Wenzel, P.L., McKinney-Freeman, S.L., Ross, S.J., Kim, P.G., Chou, S.S., Yoshimoto, M., Yoder, M.C., and Daley, G.Q. (2014). Effect of developmental stage of HSC and recipient on transplant outcomes. Dev. Cell *29*, 621–628.

Baron, C.S., Kester, L., Klaus, A., Boisset, J.C., Thambyrajah, R., Yvernogeau, L., Kouskoff, V., Lacaud, G., van Oudenaarden, A., and Robin, C. (2018). Single-cell transcriptomics reveal the dynamic of haematopoietic stem cell production in the aorta. Nat. Commun. *9*, 2517.

Batsivari, A., Rybtsov, S., Souilhol, C., Binagui-Casas, A., Hills, D., Zhao, S., Travers, P., and Medvinsky, A. (2017). Understanding hematopoietic stem cell development through functional correlation of their proliferative status with the intra-aortic cluster architecture. Stem Cell Reports *8*, 1549–1562.

Beaudin, A.E., Boyer, S.W., Perez-Cunningham, J., Hernandez, G.E., Derderian, S.C., Jujjavarapu, C., Aaserude, E., MacKenzie, T., and Forsberg, E.C. (2016). A transient developmental hematopoietic stem cell gives rise to innate-like B and T cells. Cell Stem Cell *19*, 768–783.

Carey, J.B., Moffatt-Blue, C.S., Watson, L.C., Gavin, A.L., and Feeney, A.J. (2008). Repertoire-based selection into the marginal zone compartment during B cell development. J. Exp. Med. *205*, 2043–2052.

Fraser, S.T., Ogawa, M., Yu, R.T., Nishikawa, S., Yoder, M.C., and Nishikawa, S. (2002). Definitive hematopoietic commitment within the embryonic vascular endothelial-cadherin(+) population. Exp. Hematol. *30*, 1070–1078.

Ghosn, E.E., Waters, J., Phillips, M., Yamamoto, R., Long, B.R., Yang, Y., Gerstein, R., Stoddart, C.A., Nakauchi, H., and Herzenberg, L.A. (2016). Fetal hematopoietic stem cell transplantation fails to fully regenerate the B-lymphocyte compartment. Stem Cell Reports *6*, 137–149.

Ghosn, E.E., Yamamoto, R., Hamanaka, S., Yang, Y., Herzenberg, L.A., Nakauchi, H., and Herzenberg, L.A. (2012). Distinct B-cell lineage commitment distinguishes adult bone marrow hematopoietic stem cells. Proc. Natl. Acad. Sci. U S A *109*, 5394–5398.

Hadland, B., and Yoshimoto, M. (2018). Many layers of embryonic hematopoiesis: new insights into B-cell ontogeny and the origin of hematopoietic stem cells. Exp. Hematol. *60*, 1–9.

Hadland, B.K., Varnum-Finney, B., Mandal, P.K., Rossi, D.J., Poulos, M.G., Butler, J.M., Rafii, S., Yoder, M.C., Yoshimoto, M., and Bernstein, I.D. (2017). A common origin for B-1a and B-2 lymphocytes in clonal pre- hematopoietic stem cells. Stem Cell Reports *8*, 1563–1572.

Hadland, B.K., Varnum-Finney, B., Poulos, M.G., Moon, R.T., Butler, J.M., Rafii, S., and Bernstein, I.D. (2015). Endothelium and NOTCH specify and amplify aorta-gonad-mesonephros-derived hematopoietic stem cells. J. Clin. Invest. *125*, 2032–2045.

Hardy, R.R., and Hayakawa, K. (1991). A developmental switch in B lymphopoiesis. Proc. Natl. Acad. Sci. U S A *88*, 11550–11554.

Hayakawa, K., Hardy, R.R., Parks, D.R., and Herzenberg, L.A. (1983). The "Ly-1 B" cell subpopulation in normal immunodefective, and autoimmune mice. J. Exp. Med. *157*, 202–218.

Inlay, M.A., Serwold, T., Mosley, A., Fathman, J.W., Dimov, I.K., Seita, J., and Weissman, I.L. (2014). Identification of multipotent progenitors that emerge prior to hematopoietic stem cells in embryonic development. Stem Cell Reports *2*, 457–472.

Kobayashi, M., Shelley, W.C., Seo, W., Vemula, S., Lin, Y., Liu, Y., Kapur, R., Taniuchi, I., and Yoshimoto, M. (2014). Functional B-1 progenitor cells are present in the hematopoietic stem cell-deficient embryo and depend on Cbfbeta for their development. Proc. Natl. Acad. Sci. U S A *111*, 12151–12156.

Kristiansen, T.A., Jaensson Gyllenback, E., Zriwil, A., Bjorklund, T., Daniel, J.A., Sitnicka, E., Soneji, S., Bryder, D., and Yuan, J. (2016). Cellular barcoding links B-1a B cell potential to a fetal hematopoietic stem cell state at the single-cell level. Immunity *45*, 346–357.

Montecino-Rodriguez, E., Fice, M., Casero, D., Berent-Maoz, B., Barber, C.L., and Dorshkind, K. (2016). Distinct genetic networks orchestrate the emergence of specific waves of fetal and adult B-1 and B-2 development. Immunity *45*, 527–539.

Rybtsov, S., Sobiesiak, M., Taoudi, S., Souilhol, C., Senserrich, J., Liakhovitskaia, A., Ivanovs, A., Frampton, J., Zhao, S., and Medvinsky, A. (2011). Hierarchical organization and early hematopoietic specification of the developing HSC lineage in the AGM region. J. Exp. Med. *208*, 1305–1315.

Yoder, M.C., Hiatt, K., Dutt, P., Mukherjee, P., Bodine, D.M., and Orlic, D. (1997). Characterization of definitive lymphohematopoietic stem cells in the day 9 murine yolk sac. Immunity *7*, 335–344.

Yoshimoto, M., Montecino-Rodriguez, E., Ferkowicz, M.J., Porayette, P., Shelley, W.C., Conway, S.J., Dorshkind, K., and Yoder, M.C. (2011). Embryonic day 9 yolk sac and intra-embryonic hemogenic endothelium independently generate a B-1 and marginal zone progenitor lacking B-2 potential. Proc. Natl. Acad. Sci. U S A *108*, 1468–1473.

Zhou, F., Li, X., Wang, W., Zhu, P., Zhou, J., He, W., Ding, M., Xiong, F., Zheng, X., Li, Z., et al. (2016). Tracing haematopoietic stem cell formation at single-cell resolution. Nature *533*, 487–492.